Ecotoxicology and Environmental Safety 191 (2020) 110223

Contents lists available at ScienceDirect

Ecotoxicology and Environmental Safety

journal homepage: www.elsevier.com/locate/ecoenv

Cytotoxicity and toxicoproteomic analyses of human lung epithelial cells exposed to extracts of atmospheric particulate matters on PTFE filters using acetone and water

Zhi-jie Tang[a], Zhao-ming Cao[a], Xue-wen Guo[a], Hong-juan Chen[b], Yi Lian[c], Wei-juan Zheng[b], Yi-jun Chen[a], Hong-zhen Lian[a,*], Xin Hu[a,**]

[a] State Key Laboratory of Analytical Chemistry for Life Science, School of Chemistry & Chemical Engineering and Center of Materials Analysis, Nanjing University, Nanjing, 210023, China
[b] State Key Laboratory of Pharmaceutical Biotechnology, School of Life Sciences, Nanjing University, Nanjing, 210023, China
[c] Department of Epidemiology, Biostatistics and Occupational Health, McGill University, QC, H3A 1A2, Canada

ARTICLE INFO

Keywords:
Particulate matters
Different extracts
Cytotoxicity
Toxicoproteomics
iTRAQ

ABSTRACT

Differences of cytotoxicity associated with exposure to different extracts of atmospheric particulate matters (PMs) are still not well characterized by in vitro toxicoproteomics. In this study, in vitro cytotoxicity assays and toxicoproteomic analyses were carried out to investigate toxic effects of PM collected using polytetrafluoroethylene (PTFE) filters extracted with acetone for $PM_{2.1}$ and water for $PM_{2.1}$ and PM_{10} on A549 human lung epithelial cells. The cytotoxicity assays based on cell viability, cell apoptosis and reactive oxygen species generation indicated that $PM_{2.1}$ extracted with acetone had the highest toxicity. iTRAQ labeling and LC-MS/MS analyses indicated that the number of differentially expressed proteins in A549 cells affected by $PM_{2.1}$ extracted with acetone was noticeably higher than that of the other two groups. Hierarchical cluster analyses showed that the influences of the extracts of $PM_{2.1}$ and PM_{10} using water on the proteome of A549 cells were similar, whereas significantly different from the effect of $PM_{2.1}$ extracted with acetone. Pathways analyses indicated that $PM_{2.1}$ extracted with acetone influenced the expression of proteins involved in 14 pathways including glycolysis/gluconeogenesis, pentose phosphate pathway, proteasome, etc. $PM_{2.1}$ extracted with water affected the expression of proteins involved in 3 pathways including non-homologous end-joining, ribosome and endocytosis. However, PM_{10} extracted with water affected the expression of proteins involved in only spliceosome pathway. The extracts of PM using different extractants to detach PM from PTFE filters influenced the cytotoxic effects of PM and the proteome of A549 cells. Therefore, extractants should be assessed carefully before the investigations on cytotoxicity to improve the compatibility of experimental results among research teams.

1. Introduction

Atmospheric particulate matters (PMs) are of great interests due to their acute and chronic adverse health effects (Boldo et al., 2006; Cheng et al., 2013; Kim et al., 2015). For example, numerous epidemiological studies have indicated that fine and ultrafine PMs are associated with respiratory diseases, cardiovascular diseases and stroke, neurodegeneration disease, diabetes, etc. (Franklin et al., 2007; Pelucchi et al., 2009; Cao et al., 2012; Chen et al., 2013a; Hoek et al., 2013; Leiva et al., 2013; Devlin et al., 2014; Zanobetti et al., 2014; Karottki et al., 2015; Kioumourtzoglou et al., 2016). PM is a complex mixture of various inorganic and organic components (Putaud et al., 2004; Hand et al., 2012; Kelly and Fussell, 2012). A number of potentially toxic elements (PTEs; e.g., lead, arsenic and cadmium) have been detected in PMs in many places (Shi et al., 2012; Massey et al., 2013; Cakmak et al., 2014; Liu et al., 2015a). Moreover, some PTEs (e.g., lead, arsenic and chromium) are more abundant in the fine PM than in the coarse PM (Voutsa and Samara, 2002; Clements et al., 2014). Different polycyclic aromatic hydrocarbons (PAHs) have been determined in PMs, including benzo [a]pyrene, benzo[a]anthracene, pyrene, naphthalene, etc. (Alves et al., 2017; Zhang et al., 2017; Wang et al., 2018). It is suggested that PAHs with lower volatility and higher molecular weight are preferentially enriched in the fine PM (Wang et al., 2018). Noticeably, the different effects of water-soluble and insoluble fractions of PM

* Corresponding author.
** Corresponding author.
E-mail addresses: hzlian@nju.edu.cn (H.-z. Lian), huxin@nju.edu.cn (X. Hu).

https://doi.org/10.1016/j.ecoenv.2020.110223
Received 11 September 2019; Received in revised form 6 January 2020; Accepted 15 January 2020

composed of various chemical components on cytotoxicity have been demonstrated (Vuong et al., 2017; Qi et al., 2019). The excess risks have also been observed in experimental animals exposed to PM. For example, the outcomes of mice exposed to concentrated $PM_{2.5}$ showed positive association with respiratory diseases and cardiometabolic diseases (Hu et al., 2017; Lopes et al., 2018).

The results of cell exposure study can provide important insights into the toxic mechanism of PM. PM has been demonstrated to be toxic to the lung tissue in mouse in vivo through intratracheal or intranasal instillation (Li et al., 2017; Maikawa et al., 2018). In vitro cells in toxicological investigations related to PM mainly included human lung and bronchial epithelial cells (Park et al., 2011; Huang et al., 2014; Sanchez-Soberon et al., 2018). In vivo and in vitro investigations of toxicity of PM are usually started from extraction of PM in order to detach PM from filters (Jeon et al., 2011; Park et al., 2011; Huang et al., 2014; Li et al., 2017; Sanchez-Soberon et al., 2018; Zhao et al., 2019). $PM_{2.5}$ samples were extracted from glass fiber filters by sonicating in sterile water (Zhao et al., 2019). $PM_{2.5}$ samples were extracted from quartz filters by sonicating in ultrapure water for 30 min (Qi et al., 2019). Samples of $PM_{10\text{-}2.5}$, $PM_{2.5\text{-}0.25}$, $PM_{0.25}$ were firstly extracted from polycarbonate filters by sonicating in deionized water for 10 min and finally freeze dried (Sanchez-Soberon et al., 2018). Samples of size-segregated PMs were firstly extracted from quartz filters by DCM/n-hexane (3:2 v/v) in a microwave-assisted extraction and finally evaporated to dryness under mild N_2 flow (Velali et al., 2016a). Interestingly, not only water-insoluble components of $PM_{2.5}$ have greater toxic effect than soluble ones on neonatal rat cardiomyocytes (Qi et al., 2019), but also PM_{10} acetone extracts were more toxic than aqueous extracts to BEAS-2B human bronchial epithelial cells (Rodriguez-Cotto et al., 2014). Such inconsistence in cytotoxicity is probably attributed to operationally defined extraction procedures extracting different chemical components from same a PM, which could bring the difficulty to explain the intrinsic toxicological responses of PM.

Proteomics can be a useful tool in assessing toxic mechanisms associated with environmental pollutants exposure (Jebali et al., 2014; Lafontaine et al., 2017; Ariganello et al., 2018). Limited data have been published on in vitro toxicoproteomic analyses of cells exposed to PMs. Complete PM consists of a solvent-soluble fraction and a solvent-insoluble fraction. These water-insoluble fraction of urban dust was largely responsible for the toxicity of urban dust in A549 human lung epithelial cells (Vuong et al., 2017). Studies showed that following exposure to steel industry PM, proteins related to redox homeostasis, metabolism, DNA damage and repair were severely impacted (Kumar et al., 2018). The heavy fuel oil particles also affected pathways in human lung cells for oxidative stress, homeostasis, biosynthetic, metabolic processes, etc. (Oeder et al., 2015). In vitro toxicoproteomic analyses of human bronchial (Park et al., 2011) and lung epithelial cells (Jeon et al., 2011; Huang et al., 2014) exposed to nanoPM extracted with dimethyl sulfoxide (DMSO) (Park et al., 2011), fine PM extracted with water (Huang et al., 2014) and coarse PM extracted with DMSO (Jeon et al., 2011) were performed to investigate cytotoxic mechanisms of PM. However, a detailed comparison of in vitro toxicoproteomics has not been performed to investigate the differences of toxic effects of PM extracted with different solvents. Therefore, toxicoproteomics should be a powerful technique to accurately compare the effects of operationally defined procedures on cytotoxicity of PM and reasonably elucidate toxic mechanisms of PM.

In previous studies, we demonstrated that in vitro proteomics was able to elucidate the mechanisms of cytotoxic effects of zinc oxide nanoparticles and PTEs (cadmium, zinc) on A549 cells (Zhao et al., 2014, 2015, 2018; Zhang et al., 2018). In the present work, size-segregated PMs were collected using polytetrafluoroethylene (PTFE) filters. Two equal parts of PM were extracted with water and acetone to detach PM from filters, respectively. Toxicoproteomic analyses of A549 cells following exposure to PM were performed using iTRAQ labeling and liquid chromatography-tandem mass spectrometer (LC-MS/MS), based on the assays of cell viability, cell apoptosis and reactive oxygen species (ROS) generation. The key objectives of this study were: (a) to investigate changes in the expression of proteins and pathways in A549 cells following exposure to PM by toxicoproteomic analyses; (b) to compare responses of A549 cells exposed to PM extracted with water and PM extracted with acetone; (c) to compare responses of A549 cells exposed to fine PM and coarse PM.

2. Materials and methods

2.1. Particulate matters sample and preparation

PMs were sampled at a platform outside the window of an office room located on the second floor in Xianlin campus of Nanjing University (118°57′ E, 32°7′ N). Samples of PM deposited on the PTFE filters were synchronously collected for 144 h using two Andersen eight stage non-viable cascade impactors (Tisch, TE-20-800, USA) at a flow rate of 28.3 L/min from May 2016 to December 2017. PM was segregated into 9 size fractions: > 9.0 μm on the first stage, 5.8–9.0 μm, 4.7–5.8 μm, 3.3–4.7 μm, 2.1–3.3 μm, 1.1–2.1 μm, 0.7–1.1 μm, 0.4–0.7 μm and < 0.4 μm on the last stage. Fine PM is detrimental because it can penetrate into the lower part of respiratory tract and reach the alveoli of lung (Huang et al., 2016). On the other hand, coarse PM deposits mainly in the trachea or primary and secondary bronchi (Londahl et al., 2006).

Two equal parts of PM deposited on PTFE filters were extracted with water and acetone, respectively. In brief, a set of four PTFE filters (< 0.4 μm, 0.4–0.7 μm, 0.7–1.1 μm and 1.1–2.1 μm) was divided into two equal parts. The other set of nine PTFE filters (< 0.4 μm, 0.4–0.7 μm, 0.7–1.1 μm, 1.1–2.1 μm, 2.1–3.3 μm, 3.3–4.7 μm, 4.7–5.8 μm, 5.8–9.0 μm and > 9.0 μm) was also divided into two equal parts. Filters were cut into pieces. One part of the $PM_{2.1}$ and PM_{10}-deposited PTFE filters were separately placed in 20 mL ultrapure water. The other part of $PM_{2.1}$-deposited PTFE filters were placed in 20 mL acetone. The samples were sonicated twice in a pre-chilled water bath for 30 min. Then the water suspensions were lyophilized, and the acetone suspension was dried with a nitrogen stream after the filters had been removed. The final particles were stored frozen at −80 °C.

2.2. Characterization of particulate matters

To analyze the contents of PM-bound elements, a Milestone ETHOS 1 (Milestone, Italy) microwave sample preparation system with temperature control was utilized to digest the PM samples. The microwave-assisted digestion procedure was listed in the previous report (Hu et al., 2013). Concentrations of elements in the resulting solution were detected by inductively coupled plasma optical emission spectrometer (ICP-OES) (PerkinElmer SCIEX, Optima 5300, USA) and inductively coupled plasma mass spectrometry (ICP-MS) (PerkinElmer SCIEX, Elan 9000, USA). The conditions of ICP-OES and ICP-MS are listed in Table S1 and Table S2, respectively. PM was characterized by a field emission scanning electron microscope coupled with energy dispersive X-ray spectroscope (SEM-EDX) (JEOL, JSM-7800F, Japan). Fourier transform infrared spectroscopy (FT-IR) analyses of the samples were carried out by an attenuated total reflection (ATR) FT-IR spectrometer (Nicolet, 6700, USA).

2.3. Cell culture and particulate matters exposure

A549 cells were purchased from Cobioer Biotech (Nanjing, China) and maintained in the complete Ham's F–12K (Kaighn's modification) (Gibco, USA) medium supplemented with 10% fetal bovine serum (FBS) (Hyclone, USA), 100 units/mL penicillin and 100 μg/mL streptomycin (Gibco, USA) in a humidified 5% carbon dioxide atmosphere at 37 °C. To prepare PM for dosing cells, PM detached from filters was re-suspended in cell culture medium (5% serum-containing F–12K). The

suspensions were dispersed by sonicating in a pre-chilled water bath for 30 min. It should be noted that the final concentration of FBS that the A549 cells were exposed to was 5% after dosing with PM.

2.4. Cell viability assay

Cell viability was determined by cell counting kit-8 (CCK-8) (Beyotime, China). Briefly, A549 cells were seeded with a density of 5000 cells/well in 96-well plates and cultured for 24 h. After removing the complete medium, the A549 cells were treated with freshly dispersed PM at the final concentrations of 1, 5, 10, 25, 50, 100, 200 μg/mL for 4, 12, 24 and 48 h. The PM suspensions were removed after exposure. The plates were washed twice with phosphate buffered saline (PBS; pH 7.4) and followed by the addition of 10 μL of the CCK-8 reagent and 100 μL of fresh medium in each well. Then the plates were incubated for 1 h at 37 °C. The supernatants were transferred to fresh plates and absorbance was measured at 450 nm by a microplate reader (ThermoFisher Scientific, Varioskan Flash, USA).

2.5. Cell apoptosis assay

Apoptosis assay of A549 cells was performed by Annexin V-FITC apoptosis detection kit (Beyotime, China). Briefly, A549 cells were seeded with a density of 1×10^5 cells/well in 12-well plates and cultured for 24 h. After removing the complete medium, the A549 cells were treated with freshly dispersed PM at the final concentrations of 50 and 100 μg/mL for 24 h. The A549 cells were then collected and resuspended using PBS buffer (pH 7.4). 1×10^5 A549 cells were taken and centrifuged at 100 g for 5 min. The supernatants were discarded, and 195 μL Annexin V-FITC binding solution, 5 μL Annexin V-FITC and 10 μL PI staining solution were added to each sample. The samples were incubated in a dark place at room temperature for 20 min and then analysed by a flow cytometer (Becton Dickinson, FACSCalibur, USA).

2.6. Reactive oxygen species assay

Intracellular reactive oxygen species (ROS) production was measured using ROS assay kit (Beyotime, China). ROS levels were determined using 2′,7′-dichlorodihydrofluorescein diacetate (DCFH-DA), a cell permeable nonfluorescent molecular probe oxidized by ROS to produce fluorescent compound 2′,7′-dichlorofluorescein (DCF) (Chen et al., 2013b; Deng et al., 2013). All cell exposure experiments were conducted at 80%–90% of cell confluence. When A549 cells reached confluence, the complete medium was removed. A549 cells were exposed to freshly dispersed PM at the final concentrations of 1, 5, 10, 25, 50, 100, 200 μg/mL for 12, 24 and 48 h. The PM suspensions were removed and then the cells were washed twice with serum-free medium. 100 μL 10 μmol/L DCFH-DA in serum-free medium was added to each well in 96-well plates, and the cells were incubated at 37 °C for 30 min. Then the DCFH-DA was removed, each well was washed twice with serum-free medium. Finally, fluorescence intensity of DCF in each well was determined by a microplate reader (ThermoFisher Scientific, Varioskan Flash, USA) with excitation and emission wavelengths of 488 nm and 525 nm, respectively.

2.7. Protein extraction, iTRAQ labeling and LC-MS/MS analyses

A549 cells were seeded with a density of 1×10^6 cells/dish in dishes with diameters of 10 cm and cultured for 24 h. Then the A549 cells were treated with freshly dispersed PM at the final concentration of 100 μg/mL for 24 h after removing the complete medium. Cell lysis was carried out using cell lysis buffer for Western and immunol precipitation (Beyotime, China). In brief, the cells were washed twice with ice-cold PBS and followed by the addition of 1 mL cell lysis buffer in ice bath. The lysates were collected after the addition of 1 mL cell lysis buffer for 3 min and then sonicated for 1 min. The lysates were centrifuged at 12,000 g for 20 min at 4 °C and supernatants were recovered. The concentrations of protein in the supernatants were determined using BCA protein assay kit (Beyotime, China). Protein samples were flash-frozen and stored at −80 °C.

For each sample, 200 μg of total protein was reduced, alkylated, trypsin-digested and then labeled with iTRAQ reagent-8 plex multiplex kit (AB Sciex, USA) according to the manufacturer's instructions. Briefly, 200 μg protein was reduced with 4 μL reducing reagent at 60 °C for 1 h. Then 2 μL cysteine-blocking reagent was added. After reaction for 10 min, the sample was centrifuged at 12,000 g for 20 min and bottom solution was discarded. Protein was digested with trypsin overnight in a mass ratio of 1:50 trypsin to protein at 37 °C. iTRAQ reagent was then added to the sample and incubation at room temperature for 2 h. Labeled samples were resuspended with mobile phase A and loaded onto a Durashell C18 column (4.6 mm × 150 mm, 5 μm). Peptides were separated after 65 min solvent gradient from 5% B to 90% B (A: 20 mM ammonium formate, B: 20 mM ammonium formate, 80% acetonitrile). A triple TOF 5600 mass spectrometer fitted with a nanospray III source (AB Sciex, USA) was utilized to acquire mass data. The conditions of mass spectrometer were programmed as follows: ion spray voltage of 2.5 kV, curtain gas of 30 PSI, m/z from 350 to 1250, accumulation time of 0.25 s.

2.8. Statistics and bioinformatics

All measurements were repeated at least three times and the data were expressed as means ± SD. Statistical analyses were conducted using SPSS 19 for Windows software package (SPSS, USA). Independent samples T test was used to detect any significant difference between the control and the treated group at 95% confidence level. One-way analysis of variance (ANOVA) was performed on cytotoxicity tests to assess whether cytotoxicity differed significantly across various treated groups. Post-hoc multiple comparisons of means were conducted using Tukey test. *$p < 0.05$ indicates significant difference compared with control group by the independent samples T test. Average values with different letters indicate significant differences among various treated groups by the Tukey test ($p < 0.05$).

ProteinPilot™ software (version 4.2) was used to process raw data against the database of homo sapiens from UniProt (https://www.uniprot.org/). The primary search parameters were listed as follows. Cysteine modified with iodoacetamide, trypsin digestion, iTRAQ quantification, instrument triple TOF 5600, biological modifications selected as ID. Peptides with a global false discovery rate (FDR) < 1% were used for proteins annotation. In order to determine the fold-changes for proteins from treatment groups, the treatment/control ratios were first calculated. The differentially expressed protein was identified on the basis of fold-change > 1.50 or < 0.67 and p-value < 0.05. Furthermore, fold-change was converted into $\log_2$ (treatment/control ratio) so that the data were continuous for hierarchical cluster analyses because there was no gap between −1.0 and 1.0 when $\log_2$ (treatment/control) was adopted. Hierarchical cluster analyses were conducted using the Perseus software. The Gene Ontology (GO) annotation for differentially expressed proteins was obtained from the DAVID bioinformatics resources version 6.8 (https://david.ncifcrf.gov/). The GO annotation contains biological process, cellular component and molecular function. The Kyoto Encyclopedia of Genes and Genomes (KEGG) (https://www.genome.jp/kegg/) was employed to analyze pathways.

3. Results and discussion

3.1. Physicochemical characterization of particulate matters

Concentrations of inorganic elements in size-segregated PMs containing Al, Ba, Ca, Cr, Fe, K, Mg, Mn, Mo, Na, Ni, Sb, Se, Sr, Ti, As, Cu, Zn, Pb, Cd and Co are listed in Table 1. The average total content of 21

Table 1
Concentrations (ng/m^3) of elements in size-segregated PMs (n = 6).

Elements	Size fractions (μm)								
	< 0.4	0.4–0.7	0.7–1.1	1.1–2.1	2.1–3.3	3.3–4.7	4.7–5.8	5.8–9.0	> 9.0
Al	63.6	70.4	61.8	106	181	280	208	312	470
Ba	2.54	3.89	8.29	8.65	10.5	12.1	7.12	11.0	15.5
Ca	386	555	383	496	822	1.28×10^3	866	1.43×10^3	2.18×10^3
Cr	1.62	1.86	1.86	1.98	2.26	2.40	1.60	2.09	3.16
Fe	140	204	193	223	332	480	269	444	681
K	92.7	204	197	140	74.7	89.0	70.1	76.5	113
Mg	29.3	41.0	37.5	62.8	90.1	118	81.2	130	264
Mn	5.17	12.6	14.0	11.6	8.22	11.3	5.83	10.2	15.8
Mo	0.752	0.785	0.671	0.638	0.769	0.687	0.703	0.474	0.769
Na	43.5	65.7	60.3	86.8	112	113	69.7	118	214
Ni	4.84	9.10	4.99	2.91	5.68	7.95	5.64	2.93	3.42
Sb	109	101	140	126	112	102	87.4	50.5	74.6
Sr	0.589	1.06	0.982	1.42	2.31	3.35	2.03	3.42	5.48
Ti	11.1	9.10	8.57	11.7	16.8	21.6	19.2	23.1	38.4
As	1.88	2.81	3.51	3.23	1.33	0.798	0.339	0.564	0.531
Cu	4.59	7.79	5.81	6.26	5.16	5.38	2.20	7.53	9.46
Zn	31.6	51.5	59.2	84.4	50.9	27.5	17.8	30.0	30.3
Pb	13.8	27.7	30.5	27.4	16.5	4.88	4.39	3.87	5.93
Cd	0.340	0.521	0.638	0.655	0.363	0.148	0.0729	0.0870	0.0740
Co	8.04	6.02	7.27	8.35	8.39	5.87	5.30	7.38	11.0
V	1.86	1.07	0.983	0.972	0.847	0.649	0.386	0.687	0.933

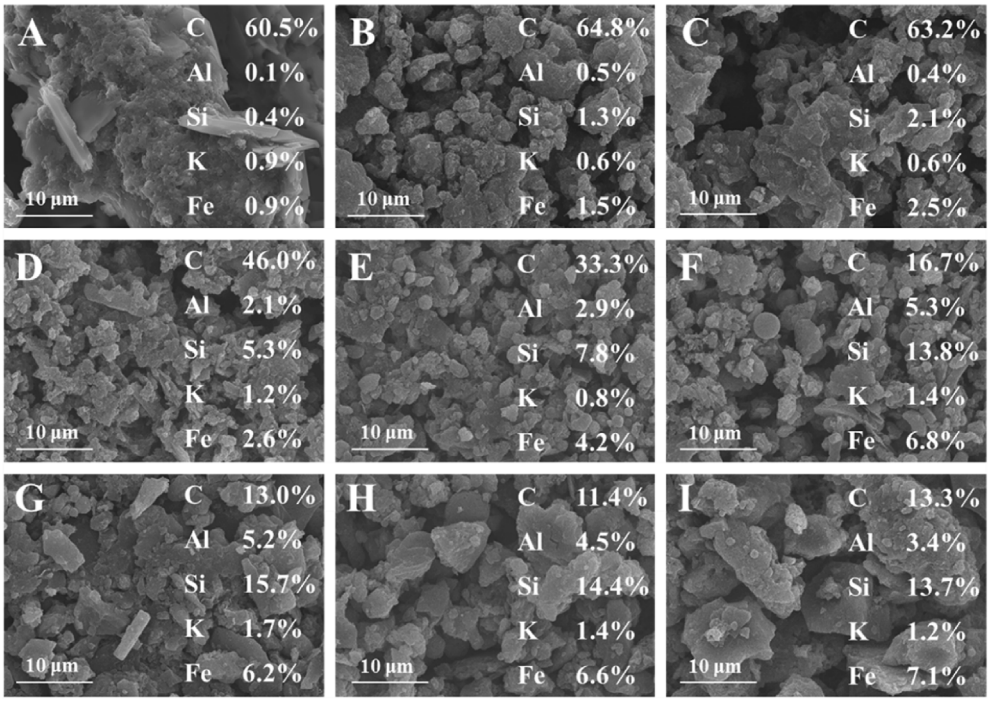

Fig. 1. SEM-EDX analyses of size-segregated PMs deposited on PTFE filters at 3000 times magnification (A: < 0.4 μm, B: 0.4–0.7 μm, C: 0.7–1.1 μm, D: 1.1–2.1 μm, E: 2.1–3.3 μm, F: 3.3–4.7 μm, G: 4.7–5.8 μm, H: 5.8–9.0 μm, I: > 9.0 μm).

elements in all fractions was 17.9 μg/m^3. The most abundant metals detected in PM were Ca, Fe and Al. The lowest level in PM was observed for Cd. The contents of crustal elements (Fe, Al, Ca, Mg and Na) decreased with decreasing PM size. Nevertheless, the smaller the PM size, the higher the concentrations of PTEs (As, Cd, Sb, Pb, Zn and V). The morphology and several elements of size-segregated PM deposited on PTFE filters at 3000 times magnification are exhibited in Fig. 1. PM was a complex mixture of particles with various size and shape, such as sphere, rod and slice. Moreover, some fine particles agglomerated into larger particles. The EDX analyses indicated that weight percentages (Wt%) of Al, Si and Fe increased with increasing PM size. However, the larger the PM size, the lower the weight percentage of C.

ATR-FT-IR spectra of size-segregated PMs are showed in Fig. 2. ATR-FT-IR spectra indicated that the structure and functional groups of $PM_{0.4\text{-}0.7}$, $PM_{0.7\text{-}1.1}$ and $PM_{1.1\text{-}2.1}$ had many similarities, which were noticeably different from those of coarse particles. As shown in ATR-FT-IR spectra of fine particles, the peak observed at 3183 cm^{-1} was assigned to O–H stretching vibration of carboxylic acids. The peak located at 3047 cm^{-1} was characterized by Ar–H stretching vibration. The peak observed at 1701 cm^{-1} was due to C=O stretching vibration. The peak observed at 1051 cm^{-1} was assigned to C–O stretching vibration. The peak located at 824 cm^{-1} was characterized by Ar–H bending vibration. The peak observed at 612 cm^{-1} was due to C–Cl. As shown in ATR-FT-IR spectra of coarse particles, the peaks located at 3520 and

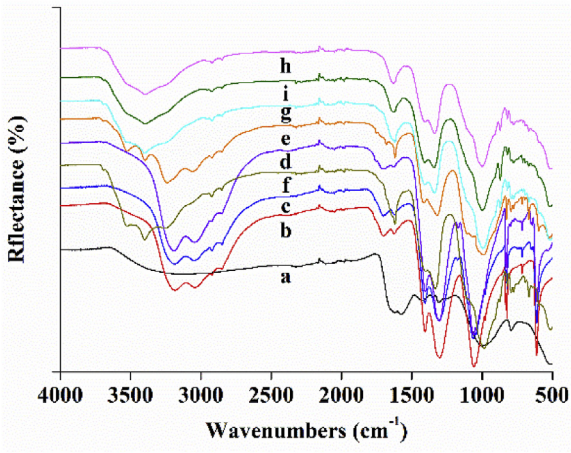

Fig. 2. ATR-FT-IR spectra of size-segregated PMs (a: < 0.4 μm, b: 0.4–0.7 μm, c: 0.7–1.1 μm, d: 1.1–2.1 μm, e: 2.1–3.3 μm, f: 3.3–4.7 μm, g: 4.7–5.8 μm, h: 5.8–9.0 μm, i: > 9.0 μm).

3407 cm^{-1} were characterized by N–H stretching vibration. The peak observed at 3237 cm^{-1} was assigned to O–H stretching vibration of alcohols. The peak located at 1000 cm^{-1} was due to Si–C group. The common peaks in fine and coarse particles observed at 2917 and 2849 cm^{-1} were characterized by C–H stretching vibration. The common peak located at 1618 cm^{-1} was assigned to C=C stretching vibration. The common peaks observed at 1403 and 1307 cm^{-1} were due to C–N and Ph-C groups, respectively. Several PAHs have been determined in $PM_{2.5}$ in some cities (Alves et al., 2017; Zhang et al., 2017). It is reported that quinones and carboxylic acids are the main components of cigarette smoke (Hoffmann and Hoffmann, 1997). Phenol is also found in the airborne PM (Mohiuddin et al., 2016). Emission from automobile engines and biomass burning are primary sources of amide (Khare et al., 2011).

3.2. Cell viability of A549 cells following exposure to particulate matters

The cell viability of A549 cells after exposure to different concentrations of PM for 4, 12, 24 and 48 h is listed in Fig. 3. Compared with the untreated control cells, no significant effects of PM on A549 cells were observed after cells exposure to 1, 5, 10, 25, 50, 100 and 200 μg/mL of PM for 4 h and 12 h. A dose-dependent decrease of cell viability was detected after 24 h and 48 h exposure of PM. The cell viability at 24 h and 48 h indicated that PM had mild cytotoxic effect on A549 cells at lower concentrations of exposure (1, 5, 10 and 25 μg/mL). However, PM was cytotoxic to A549 cells at higher levels of exposure (50, 100 and 200 μg/mL), where they were capable of reducing cell viability significantly. Viability of A549 cells affected by PM extracted with water was remarkably higher than that of A549 cells affected by PM extracted with acetone at higher levels of exposure (100 and 200 μg/mL). In addition, viability of A549 cells affected by $PM_{2.1}$ extracted with water was noticeably lower than that of A549 cells affected by PM_{10} after 24 h and 48 h at higher levels of exposure (100 and 200 μg/mL). The cell viability decreased with increasing periods of exposure and reached the lowest values at 48 h of exposure.

PM_{10} acetone extracts were more toxic than aqueous extracts to BEAS-2B human bronchial epithelial cells (Rodriguez-Cotto et al., 2014). The cytotoxicity of $PM_{0.49\text{-}0.97}$ to mitochondrial dehydrogenase in MRC-5 human fetal lung fibroblast was the highest among six water-soluble fractions of size-segregated PMs (< 0.49, 0.49–0.97, 0.97–1.5, 1.5–3.0, 3.0–7.2 and > 7.2 μm) (Velali et al., 2016b). $PM_{0.2}$ had the highest toxic potency in four size ranges ($PM_{10\text{-}2.5}$, $PM_{2.5\text{-}1}$, $PM_{1\text{-}0.2}$ and $PM_{0.2}$) in RAW264.7 macrophages (Jalava et al., 2015). In general, the in vitro responses of cells to PM are related not only to size but also to composition of PM.

3.3. Cell apoptosis of A549 cells following exposure to particulate matters

The apoptosis analyses of A549 cells after exposure to PM for 24 h are exhibited in Fig. 4 (I). PM with concentrations of 50 and 100 μg/mL induced significantly A549 cell apoptosis compared with the untreated control A549 cells. Apoptosis of A549 cells induced by 100 μg/mL PM was higher than that of A549 cells induced by 50 μg/mL PM. Apoptosis of A549 cells induced by PM extracted with water was remarkably lower than that of A549 cells induced by PM extracted with acetone. It was observed that apoptosis of A549 cells induced by $PM_{2.1}$ was significantly higher than that of A549 cells induced by PM_{10}.

Acetone extracts of cooking oil fume-derived $PM_{2.5}$ induced apoptosis of primary fetal alveolar type II epithelial cells through endoplasmic reticulum stress pathway and increment of oxidative stress (Liu et al., 2015b). Water-insoluble fraction of PM_{10} was able to induce oxidative DNA damage and apoptosis of A549 human lung epithelial cells at 24 h (Yi et al., 2014). Insoluble components of PM were able to elicit the highest cytotoxic responses in RAW 264.7 mouse macrophages after 24 h (Jalava et al., 2008).

3.4. Reactive oxygen species generation in A549 cells following exposure to particulate matters

The ROS generation in A549 cells after exposure to various concentrations of PM for 12, 24 and 48 h is showed in Fig. 4 (II-IV). The DCF fluorescence intensity was expressed as the ratio (fold change) between the exposed cells and the control cells. A dose-dependent increase of intracellular ROS generation was observed for $PM_{2.1}$ extracted with acetone and PM_{10} extracted with water. At 12 h of exposure, the DCF fluorescence intensities in A549 cells induced by $PM_{2.1}$ extracted with acetone and PM_{10} extracted with water were significantly higher compared with the untreated control cells at higher levels of exposure. Furthermore, at 24 h and 48 h of exposure, the DCF fluorescence intensities in A549 cells induced by $PM_{2.1}$ extracted with acetone and PM_{10} extracted with water were remarkably higher compared with the control cells at higher levels of exposure. DCF fluorescence intensities in A549 cells induced by $PM_{2.1}$ extracted with acetone were significantly higher than those in A549 cells induced by $PM_{2.1}$ extracted with water at higher levels of exposure (50, 100 and 200 μg/mL). In addition, DCF fluorescence intensities in A549 cells induced by PM_{10} extracted with water were significantly higher than those in A549 cells induced by $PM_{2.1}$ extracted with water at higher levels of exposure (50, 100 and 200 μg/mL). The DCF fluorescence intensities in A549 cells induced by PM_{10} extracted with water reached peak values at 12 h of exposure and dropped after 24 h. The DCF fluorescence intensities in A549 cells induced by $PM_{2.1}$ extracted with acetone increased with increasing periods of exposure and reached peak values at 48 h of exposure.

Oxidative stress related gene networks in BALB/c 3T3 A31-1-1 cells were impacted by $PM_{2.5}$ acetone extracts (Vaccari et al., 2015). A lot of soluble metals and organic compounds in PM remarkably affected the production of ROS in NR8383 rat alveolar macrophages (Heo et al., 2015). The highest redox activity was found for fine PM (0.15–2.5 μm) in three size fractions (2.5–10, 0.15–2.5, < 0.2 μm) (Akhtar et al., 2014). It is reported that a negative association between redox activity of PM and MTT-reduction activity in RAW 264.7 murine macrophages was found (Steenhof et al., 2011).

3.5. Changes in the expression of proteins in A549 cells following exposure to particulate matters

iTRAQ labeling and LC-MS/MS analyses of all the samples identified approximately a total of 4036 proteins that had one or more unique peptides per sample. These proteins were used for all subsequent bioinformatics analyses. The distribution of total, up-regulated and down-regulated differentially expressed proteins (DEPs) in A549 cells after exposure to PM for 24 h is illustrated in three Venn diagrams,

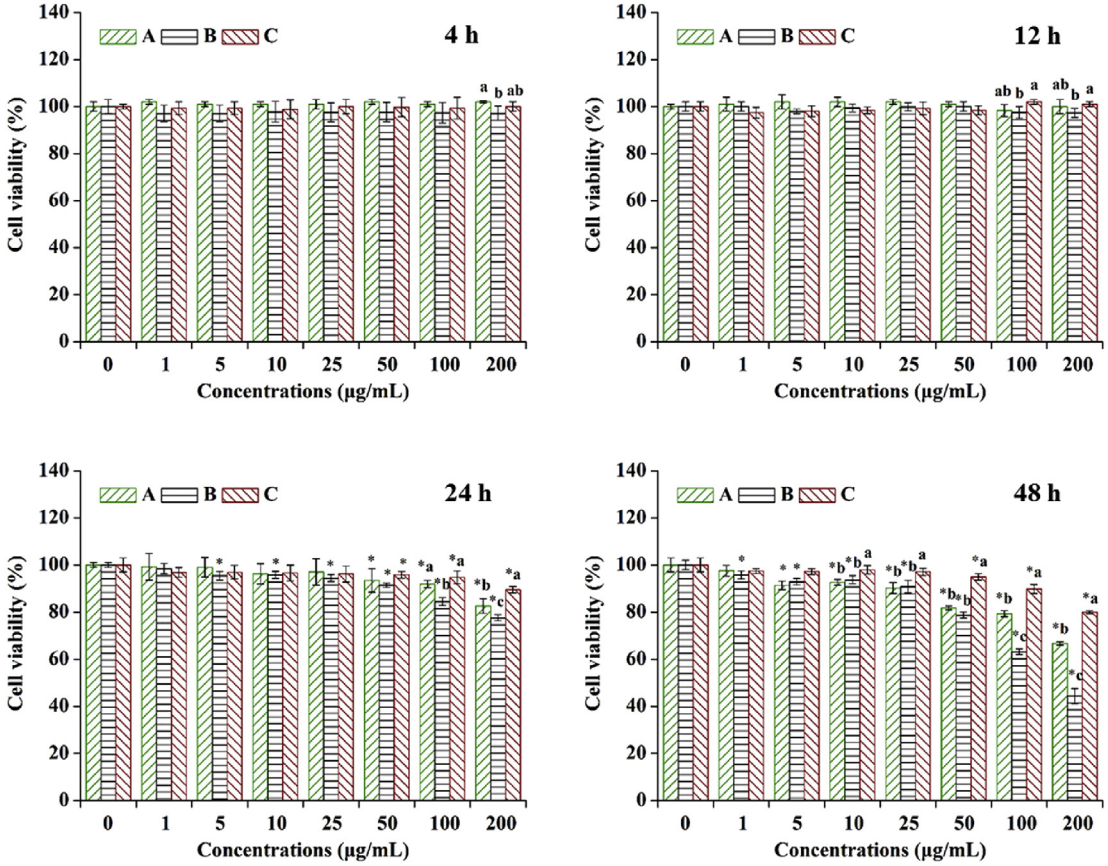

Fig. 3. Cell viability (%) of A549 cells after exposure to PM for 4, 12, 24 and 48 h (A: $PM_{2.1}$ extracted with water, B: $PM_{2.1}$ extracted with acetone, C: PM_{10} extracted with water, n = 6). *p < 0.05 indicates significant difference compared with control group by the independent samples T test. Average values with different letters indicate significant differences among various treated groups by the Tukey test (p < 0.05).

respectively (Fig. S1). The number of DEPs in A549 cells affected by $PM_{2.1}$ extracted with acetone (206) was remarkably higher than that of DEPs affected in other two groups. However, the difference between number of DEPs affected by $PM_{2.1}$ (76) and PM_{10} (88) extracted with water was subtle. The number of down-regulated DEPs (47, 152 and 50) was higher than that of up-regulated DEPs (29, 54 and 38) in the three sets, respectively. As shown in Figs. S1, 8 common total DEPs were found in the three groups. Most of common DEPs in the three groups were changed in the same direction but varying in magnitude. However, KHSRP protein was up-regulated in the A549 cells affected by PM extracted with water but down-regulated in the A549 cells affected by $PM_{2.1}$ extracted with acetone.

Hierarchical cluster analyses were performed to visually compare alterations in the proteome of A549 cells after exposure to PM for 24 h (Fig. 5). The results based on DEPs identified by LC-MS/MS showed that $PM_{2.1}$ and PM_{10} extracted with water formed a cluster that was separated from $PM_{2.1}$ extracted with acetone. Such findings indicated that $PM_{2.1}$ and PM_{10} extracted with water influenced the proteome of A549 cells similarly, whereas their effects were different from effect of $PM_{2.1}$ extracted with acetone. The DEPs in Fig. 5 appeared to form six interesting clusters (I-VI). Cluster I was dominated by proteins that were remarkably increased in expression by $PM_{2.1}$ extracted with acetone but increased or decreased by PM extracted with water. Proteins in cluster I were found to be involved in biological processes of gene expression, mRNA splicing, cell-cell adhesion, etc. Cluster II was a few proteins that were strongly down regulated by PM_{10} extracted with water and weakly down regulated or up regulated by $PM_{2.1}$ extracted with water. Proteins in cluster II were found to be involved in biological processes of protein phosphorylation. Cluster III was a small group of proteins that were noticeably down regulated by $PM_{2.1}$ extracted with acetone. Proteins in cluster III were involved in biological processes of negative regulation of hydrogen peroxide-induced cell death, activation of protein kinase B activity, response to reactive oxygen species, etc. Cluster IV showed that PM extracted with water generally increased expression of proteins, while $PM_{2.1}$ extracted with acetone generally decreased their expression. Proteins in cluster IV were involved in biological processes of regulation of mRNA stability, oxidation-reduction process, response to reactive oxygen species, etc. Cluster V was composed of proteins that were generally decreased by $PM_{2.1}$ extracted with water and decreased or increased by PM_{10} extracted with water. Proteins in cluster V were related to biological processes of translational initiation, lipid biosynthetic process, rRNA processing, etc. Cluster VI exhibited that proteins were strongly decreased in expression by $PM_{2.1}$ extracted with acetone but weakly decreased or increased by PM extracted with water. Proteins in cluster VI were involved in biological processes of gluconeogenesis, NIK/NF-kappaB signaling, tumor necrosis factor-mediated signaling pathway, etc.

3.6. Effects of particulate matters on various pathways in A549 cells

Pathways that were impacted by the PM for 24 h based on the total DEPs in A549 cells are listed in Table 2. The effects of PM on pathways in A549 cells were PM-specific. The number of pathways in A549 cells affected by $PM_{2.1}$ extracted with acetone was noticeably higher than that of pathways affected in the other two groups. In addition, the number of pathways in A549 cells affected by PM_{10} extracted with water was lower than that of pathways in A549 cells affected by $PM_{2.1}$ extracted with water. Results of KEGG pathways analyses in Table 2 revealed that $PM_{2.1}$ extracted with acetone influenced the expression of proteins involved in 14 pathways including proteasome, proteoglycans

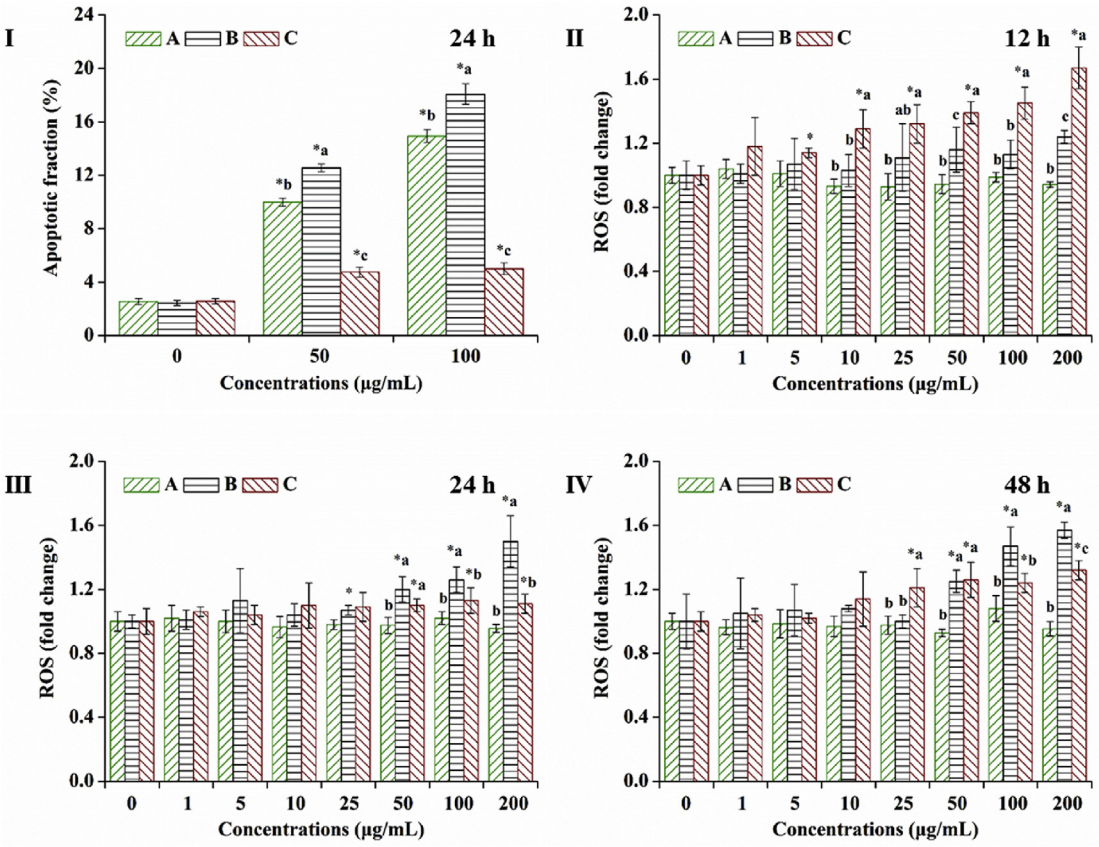

Fig. 4. Apoptosis analyses (I) of A549 cells and ROS generation (II, III and IV) in A549 cells after exposure to PM (A: $PM_{2.1}$ extracted with water, B: $PM_{2.1}$ extracted with acetone, C: PM_{10} extracted with water, n = 6). *p < 0.05 indicates significant difference compared with control group by the independent samples T test. Average values with different letters indicate significant differences among various treated groups by the Tukey test (p < 0.05).

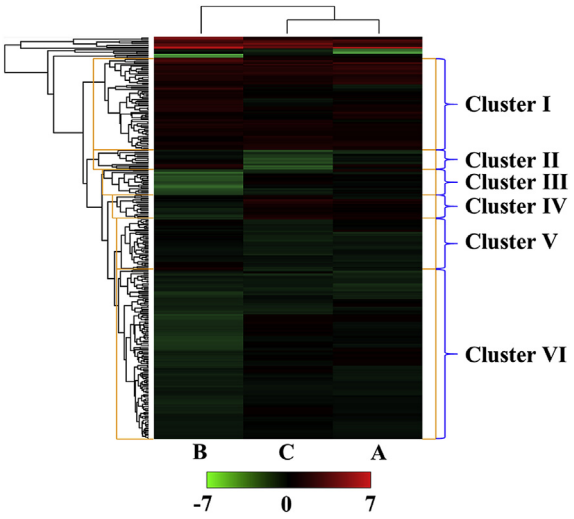

Fig. 5. Hierarchical cluster analyses of differentially expressed proteins in A549 cells after exposure to PM for 24 h (A: $PM_{2.1}$ extracted with water, B: $PM_{2.1}$ extracted with acetone, C: PM_{10} extracted with water). Values for each protein (rows) in all samples (columns) analysed are colored based on the fold changes, high (red) and low (green) values are showed in the color bar at the bottom. (For interpretation of the references to color in this figure legend, the reader is referred to the Web version of this article.)

in cancer, protein processing in endoplasmic reticulum, etc. It was observed that $PM_{2.1}$ extracted with water affected the expression of proteins involved in 3 pathways including non-homologous end-joining, ribosome and endocytosis. However, PM_{10} extracted with water affected the expression of proteins involved in only spliceosome pathway.

Table 2
KEGG pathways that were impacted by the PM for 24 h based on the differentially expressed proteins in A549 cells. All the specified pathways are statistically enriched (p-value < 0.05).

Pathways	Count	%	p-value
$PM_{2.1}$ extracted with water			
Non-homologous end-joining	3	4.48	2.23×10^{-3}
Ribosome	5	7.46	6.41×10^{-3}
Endocytosis	5	7.46	4.27×10^{-2}
$PM_{2.1}$ extracted with acetone			
Carbon metabolism	13	6.95	3.52×10^{-7}
Protein processing in endoplasmic reticulum	15	8.02	7.81×10^{-7}
Biosynthesis of amino acids	9	4.81	2.50×10^{-5}
Proteasome	7	3.74	8.45×10^{-5}
Glycolysis/Gluconeogenesis	6	3.21	5.26×10^{-3}
Antigen processing and presentation	6	3.21	8.92×10^{-3}
Proteoglycans in cancer	9	4.81	1.94×10^{-2}
Focal adhesion	9	4.81	2.27×10^{-2}
Tryptophan metabolism	4	2.14	2.94×10^{-2}
Phenylalanine, tyrosine, tryptophan biosynthesis	3	1.60	4.15×10^{-2}
Arginine biosynthesis	3	1.60	4.40×10^{-2}
Pentose phosphate pathway	3	1.60	4.52×10^{-2}
Metabolic pathways	28	15.0	4.58×10^{-2}
Amino sugar and nucleotide sugar metabolism	4	2.14	4.67×10^{-2}
PM_{10} extracted with water			
Spliceosome	4	5.48	3.40×10^{-2}

The KEGG maps are showed in Figs. S3–S20 to highlight the critical pathways in A549 cells that were affected by PM for 24 h. Glycolysis is a preferentially pathway that metabolizes glucose to pyruvate in cytoplasm and generates ATP energy for proliferation and growth for most

cancer cells (Choi et al., 2013; Li et al., 2015). Gluconeogenesis produces glucose from noncarbohydrate precursors and is necessary for cancer cells growth (Zhang et al., 2014). The pentose phosphate pathway, a branch of glycolysis, is proved to be an important pathway in cancer growth and survival (Jiang et al., 2014). The ubiquitin-proteasome system is vital for degradation of most proteins that regulate cell signal transduction, growth, apoptosis, etc. (Huang et al., 2017). Changed expression of proteoglycans on cancer cell membranes influences cell signaling, adhesion, growth, survival, etc. (Theocharis et al., 2015). The endoplasmic reticulum is involved in protein synthesis, modification and folding. Non-homologous DNA end-joining is one of major pathways for repairing double-strand DNA breaks in eukaryotic cells (Lieber, 2010). Ribosome biogenesis is the process that making ribosomes in the nucleolus and cytoplasm to sustain cell homeostasis and survival (Chen and Ioannou, 1999). Endocytosis is one of pathways that nanoparticles absorbed into cells (Oh and Park, 2014). Spliceosomes are dynamic structures in the nucleus and are changed when responding to cellular environment, particularly associated with the transcriptional state of the cell (Wong et al., 2013).

3.7. Gene ontology analyses of differentially expressed proteins in A549 cells following exposure to particulate matters

The distribution of biological processes, cellular components, molecular function that were impacted by PM for 24 h based on the total, up-regulated and down-regulated DEPs in A549 cells is showed in nine Venn diagrams, respectively (Figs. S21–S23). The number of biological processes (86), cellular components (55) and molecular function (50) in A549 cells affected by $PM_{2.1}$ extracted with acetone was noticeably higher than that of biological processes, cellular components and molecular function affected in the other two groups. However, the differences between number of biological processes, cellular components and molecular function affected by $PM_{2.1}$ (21, 25 and 12) and PM_{10} extracted with water (23, 21 and 14) were subtle but distinguishable. The number of biological processes, cellular components and molecular function based on the down-regulated DEPs was higher than that of biological processes, cellular components and molecular function based on the up-regulated DEPs in the three sets, respectively. The number of DEPs affected by $PM_{2.1}$ extracted with acetone in the common biological processes, cellular components and molecular function was the highest (Figs. S24–S26). However, no significantly difference was found between the number of DEPs affected by $PM_{2.1}$ and PM_{10} extracted with water in the common biological processes, cellular components and molecular function. Two common biological processes based on the total DEPs including glycogen catabolic process and cell-cell adhesion. Twelve common cellular components based on the total DEPs including nucleus, nucleoplasm, nucleolus, membrane, intracellular ribonucleoprotein complex, etc. Five common molecular function based on the total DEPs including RNA binding, protein binding, poly(A) RNA binding, cadherin binding involved in cell-cell adhesion and ATP binding. Glucose/glycogen metabolism is a vital metabolic pathway affecting cellular proliferation and survival against environmental stresses (Ha et al., 2015). Cell-cell adhesion is related to all respects of tissue morphogenesis, such as regulation of cell shape and movement (Takeichi, 1995; Gumbiner, 2005).

4. Conclusions

To our knowledge, this is the first investigation that used cytotoxicity assays and toxicoproteomic analyses to evaluate toxic effects of different extracts of particulate matters collected using PTFE filter on cells in vitro. Both cytotoxicity assays and toxicoproteomic analyses consistently indicated that the toxicity of $PM_{2.1}$ extracted with acetone was the highest. In addition, the toxicity of PM_{10} extracted with water was lower than that of $PM_{2.1}$ extracted with water. It is suggested that in vitro responses of cells to PM are related not only to size but also to composition of PM. The results reveal that different extraction solvents to detach PM from the filters influence the cytotoxicity of PM and the proteome of cells. Therefore, it is proposed that novel approaches of PM sampling and exposure should be developed to achieve low disturbance and accurate in situ exposure.

Author contribution section

Z. J. Tang: Investigation, Methodology, Formal analysis, Data Curation, Visualization, Writing - Original Draft, Z. M. Cao: Investigation, Formal analysis, Data Curation, Visualization, X. W. Guo, H. J. Chen and Y. J. Chen: Formal analysis, Visualization, Resources, Y. Lian and X. Hu: Formal analysis, Visualization, Resources, Writing - Review & Editing, W. J. Zheng and H. Z. Lian: Conceptualization, Methodology, Resources, Project administration, Supervision, Funding acquisition, Writing - Review & Editing.

Declaration of competing interest

The authors declare that they have no conflict of interest.

Acknowledgements

This work was supported by the National Natural Science Foundation of China (91643105, 21577057, 21874065), and the Natural Science Foundation of Jiangsu Province (BK20171335).

Appendix A. Supplementary data

Supplementary data to this article can be found online at https://doi.org/10.1016/j.ecoenv.2020.110223.

References

Akhtar, U.S., Rastogi, N., McWhinney, R.D., Urch, B., Chow, C.W., Evans, G.J., Scott, J.A., 2014. The combined effects of physicochemical properties of size-fractionated ambient particulate matter on in vitro toxicity in human A549 lung epithelial cells. Toxicol. Rep. 1, 145–156.

Alves, C.A., Vicente, A.M., Custodio, D., Cerqueira, M., Nunes, T., Pio, C., Lucarelli, F., Calzolai, G., Nava, S., Diapouli, E., Eleftheriadis, K., Querol, X., Bandowe, B.A.M., 2017. Polycyclic aromatic hydrocarbons and their derivatives (nitro-PAHs, oxygenated PAHs, and azaarenes) in $PM_{2.5}$ from Southern European cities. Sci. Total Environ. 595, 494–504.

Ariganello, M.B., Das, D.D., Breznan, D., MacKinnon-Roy, C., Elisma, F., Khanchi, A., Vincent, R., Kumarathasan, P., 2018. A matrix-assisted laser desorption ionization-time-of-flight-time-of-flight-mass spectrometry-based toxicoproteomic screening method to assess in vitro particle potencies. J. Appl. Toxicol. 38, 1302–1315.

Boldo, E., Medina, S., LeTertre, A., Hurley, F., Mucke, H.G., Ballester, F., Aguilera, I., Eilstein, D., 2006. Apheis: health impact assessment of long-term exposure to $PM_{2.5}$ in 23 European cities. Eur. J. Epidemiol. 21, 449–458.

Cakmak, S., Dales, R., Kauri, L.M., Mahmud, M., Van Ryswyk, K., Vanos, J., Liu, L., Kumarathasan, P., Thomson, E., Vincent, R., Weichenthal, S., 2014. Metal composition of fine particulate air pollution and acute changes in cardiorespiratory physiology. Environ. Pollut. 189, 208–214.

Cao, J.J., Xu, H.M., Xu, Q., Chen, B.H., Kan, H.D., 2012. Fine particulate matter constituents and cardiopulmonary mortality in a heavily polluted Chinese city. Environ. Health Perspect. 120, 373–378.

Chen, F.W., Ioannou, Y.A., 1999. Ribosomal proteins in cell proliferation and apoptosis. Int. Rev. Immunol. 18, 429–448.

Chen, H., Burnett, R.T., Kwong, J.C., Villeneuve, P.J., Goldberg, M.S., Brook, R.D., van Donkelaar, A., Jerrett, M., Martin, R.V., Brook, J.R., Copes, R., 2013a. Risk of incident diabetes in relation to long-term exposure to fine particulate matter in Ontario, Canada. Environ. Health Perspect. 121, 804–810.

Chen, S.T., Lin, C.C., Liu, Y.S., Lin, C., Hung, P.T., Jao, C.W., Lin, P.H., 2013. Airborne particulate collected from central Taiwan induces DNA strand breaks, Poly(ADP-ribose) polymerase-1 activation, and estrogen-disrupting activity in human breast carcinoma cell lines. J. Environ. Sci. Health A 48, 173–181.

Cheng, Z., Jiang, J.K., Fajardo, O., Wang, S.X., Hao, J.M., 2013. Characteristics and health impacts of particulate matter pollution in China (2001-2011). Atmos. Environ. 65, 186–194.

Choi, S.Y.C., Collins, C.C., Gout, P.W., Wang, Y.Z., 2013. Cancer-generated lactic acid: a regulatory, immunosuppressive metabolite? J. Pathol. 230, 350–355.

Clements, N., Eav, J., Xie, M.J., Hannigan, M.P., Miller, S.L., Navidi, W., Peel, J.L., Schauer, J.J., Shafer, M.M., Milford, J.B., 2014. Concentrations and source insights for trace elements in fine and coarse particulate matter. Atmos. Environ. 89,

373–381.
Deng, X.B., Zhang, F., Rui, W., Long, F., Wang, L.J., Feng, Z.H., Chen, D.L., Ding, W.J., 2013. $PM_{2.5}$-induced oxidative stress triggers autophagy in human lung epithelial A549 cells. Toxicol. In Vitro 27, 1762–1770.
Devlin, R.B., Smith, C.B., Schmitt, M.T., Rappold, A.G., Hinderliter, A., Graff, D., Carraway, M.S., 2014. Controlled exposure of humans with metabolic syndrome to concentrated ultrafine ambient particulate matter causes cardiovascular effects. Toxicol. Sci. 140, 61–72.
Franklin, M., Zeka, A., Schwartz, J., 2007. Association between $PM_{2.5}$ and all-cause and specific-cause mortality in 27 US communities. J. Expo. Sci. Environ. Epidemiol. 17, 279–287.
Gumbiner, B.M., 2005. Regulation of cadherin-mediated adhesion in morphogenesis. Nat. Rev. Mol. Cell Biol. 6, 622–634.
Ha, J., Guan, K.L., Kim, J., 2015. AMPK and autophagy in glucose/glycogen metabolism. Mol. Asp. Med. 46, 46–62.
Hand, J.L., Schichtel, B.A., Pitchford, M., Malm, W.C., Frank, N.H., 2012. Seasonal composition of remote and urban fine particulate matter in the United States. J. Geophys. Res. 117, D05209.
Heo, J., Antkiewicz, D.S., Shafer, M.M., Perkins, D.A.K., Sioutas, C., Schauer, J.J., 2015. Assessing the role of chemical components in cellular responses to atmospheric particle matter (PM) through chemical fractionation of PM extracts. Anal. Bioanal. Chem. 407, 5953–5963.
Hoek, G., Krishnan, R.M., Beelen, R., Peters, A., Ostro, B., Brunekreef, B., Kaufman, J.D., 2013. Long-term air pollution exposure and cardio- respiratory mortality: a review. Environ. Health 12, 43.
Hoffmann, D., Hoffmann, I., 1997. The changing cigarette, 1950-1995. J. Toxicol. Environ. Health 50, 307–364.
Hu, X., Ding, Z.H., Zhang, Y., Sun, Y.Y., Wu, J.C., Chen, Y.J., Lian, H.Z., 2013. Size distribution and source apportionment of airborne metallic elements in Nanjing, China. Aerosol Air Qual. Res. 13, 1796–1806.
Hu, Z.Y., Chen, M.J., Zhou, H.F., Tharakan, A., Wang, X.K., Qiu, L.L., Liang, S., Qin, X.B., Zhang, Y.H., Wang, W.J., Xu, Y.Y., Ying, Z.K., 2017. Inactivation of TNF/LT locus alters mouse metabolic response to concentrated ambient $PM_{2.5}$. Toxicology 390, 100–108.
Huang, Q.Y., Zhang, J., Peng, S.Y., Tian, M.P., Chen, J.S., Shen, H.Q., 2014. Effects of water soluble $PM_{2.5}$ extracts exposure on human lung epithelial cells (A549): a proteomic study. J. Appl. Toxicol. 34, 675–687.
Huang, W., Yuan, X., Sun, T., Fan, S.J., Wang, J., Zhou, Q., Guo, W., Ran, F.X., Ge, Z.M., Yang, H.Y., Li, R.T., Cui, J.R., 2017. Proteasome inhibitor YSY01A abrogates constitutive STAT3 signaling via down-regulation of Gp130 and JAK2 in human A549 lung cancer cells. Front. Pharmacol. 8, 476.
Huang, X., Betha, R., Tan, L.Y., Balasubramanian, R., 2016. Risk assessment of bioaccessible trace elements in smoke haze aerosols versus urban aerosols using simulated lung fluids. Atmos. Environ. 125, 505–511.
Jalava, P., Wang, Q., Kuuspalo, K., Ruusunen, J., Hao, L., Fang, D., Vaisanen, O., Ruuskanen, A., Sippula, O., Happo, M., Uski, O., Kasurinen, S., Torvela, T., Koponen, H., Lehtinen, K., Komppula, M., Gu, C., Jokiniemi, J., Hirvonen, M.R., 2015. Day and night variation in chemical composition and toxicological responses of size segregated urban air PM samples in a high air pollution situation. Atmos. Environ. 120, 427–437.
Jalava, P.I., Salonen, R.O., Pennanen, A.S., Happo, M.S., Penttinen, P., Halinen, A.I., Sillanpaa, M., Hillamo, R., Hirvonen, M.R., 2008. Effects of solubility of urban air fine and coarse particles on cytotoxic and inflammatory responses in RAW 264.7 macrophage cell line. Toxicol. Appl. Pharmacol. 229, 146–160.
Jebali, J., Chicano-Galvez, E., Fernandez-Cisnal, R., Banni, M., Chouba, L., Boussetta, H., Lopez-Barea, J., Alhama, J., 2014. Proteomic analysis in caged Mediterranean crab (Carcinus maenas) and chemical contaminant exposure in Teboulba Harbour, Tunisia. Ecotoxicol. Environ. Saf. 100, 15–26.
Jeon, Y.M., Son, B.S., Lee, M.Y., 2011. Proteomic identification of the differentially expressed proteins in human lung epithelial cells by airborne particulate matter. J. Appl. Toxicol. 31, 45–52.
Jiang, P., Du, W.J., Wu, M.A., 2014. Regulation of the pentose phosphate pathway in cancer. Protein Cell 5, 592–602.
Karottki, D.G., Spilak, M., Frederiksen, M., Andersen, Z.J., Madsen, A.M., Ketzel, M., Massling, A., Gunnarsen, L., Moller, P., Loft, S., 2015. Indoor and outdoor exposure to ultrafine, fine and microbiologically derived particulate matter related to cardiovascular and respiratory effects in a panel of elderly urban citizens. Int. J. Environ. Res. Public Health 12, 1667–1686.
Kelly, F.J., Fussell, J.C., 2012. Size, source and chemical composition as determinants of toxicity attributable to ambient particulate matter. Atmos. Environ. 60, 504–526.
Khare, P., Baruah, B.P., Rao, P.G., 2011. Water-soluble organic compounds (WSOCs) in $PM_{2.5}$ and PM_{10} at a subtropical site of India. Tellus B 63, 990–1000.
Kim, K.H., Kabir, E., Kabir, S., 2015. A review on the human health impact of airborne particulate matter. Environ. Int. 74, 136–143.
Kioumourtzoglou, M.A., Schwartz, J.D., Weisskopf, M.G., Melly, S.J., Wang, Y., Dominici, F., Zanobetti, A., 2016. Long-term $PM_{2.5}$ exposure and neurological hospital admissions in the northeastern United States. Environ. Health Perspect. 124, 23–29.
Kumar, S.S., Muthuselvam, P., Pugalenthi, V., Subramanian, N., Ramkumar, K.M., Suresh, T., Suzuki, T., Rajaguru, P., 2018. Toxicoproteomic analysis of human lung epithelial cells exposed to steel industry ambient particulate matter (PM) reveals possible mechanism of PM related carcinogenesis. Environ. Pollut. 239, 483–492.
Lafontaine, A., Baiwir, D., Joaquim-Justo, C., De Pauw, E., Lemoine, S., Boulange-Lecomte, C., Forget-Leray, J., Thome, J.P., Gismondi, E., 2017. Proteomic response of Macrobrachium rosenbergii hepatopancreas exposed to chlordecone: identification of endocrine disruption biomarkers? Ecotoxicol. Environ. Saf. 141, 306–314.
Leiva, M.A., Santibanez, D.A., Ibarra, S., Matus, P., Seguel, R., 2013. A five-year study of particulate matter ($PM_{2.5}$) and cerebrovascular diseases. Environ. Pollut. 181, 1–6.
Li, R.J., Zhao, L.F., Zhang, L., Chen, M.H., Shi, J., Dong, C., Cai, Z.W., 2017. Effects of ambient $PM_{2.5}$ and 9-nitroanthracene on DNA damage and repair, oxidative stress and metabolic enzymes in the lungs of rats. Toxicol. Res. 6, 654–663.
Li, X.B., Gu, J.D., Zhou, Q.H., 2015. Review of aerobic glycolysis and its key enzymes - new targets for lung cancer therapy. Thorac. Cancer 6, 17–24.
Lieber, M.R., 2010. The mechanism of double-strand DNA break repair by the non-homologous DNA end-joining pathway. Annu. Rev. Biochem. 79, 181–211.
Liu, X.T., Zhai, Y.B., Zhu, Y., Liu, Y.N., Chen, H.M., Li, P., Peng, C., Xu, B.B., Li, C.T., Zeng, G.M., 2015a. Mass concentration and health risk assessment of heavy metals in size-segregated airborne particulate matter in Changsha. Sci. Total Environ. 517, 215–221.
Liu, Y., Chen, Y.Y., Cao, J.Y., Tao, F.B., Zhu, X.X., Yao, C.J., Chen, D.J., Che, Z., Zhao, Q.H., Wen, L.P., 2015b. Oxidative stress, apoptosis, and cell cycle arrest are induced in primary fetal alveolar type II epithelial cells exposed to fine particulate matter from cooking oil fumes. Environ. Sci. Pollut. Res. 22, 9728–9741.
Londahl, J., Pagels, J., Swietlicki, E., Zhou, J.C., Ketzel, M., Massling, A., Bohgard, M., 2006. A set-up for field studies of respiratory tract deposition of fine and ultrafine particles in humans. J. Aerosol Sci. 37, 1152–1163.
Lopes, T.D.M., Groth, E.E., Veras, M., Furuya, T.K., Costa, N.D.X., Ribeiro, G., Lopes, F.D., de Almeida, F.M., Cardoso, W.V., Saldiva, P.H.N., Chammas, R., Mauad, T., 2018. Pre- and postnatal exposure of mice to concentrated urban $PM_{2.5}$ decreases the number of alveoli and leads to altered lung function at an early stage of life. Environ. Pollut. 241, 511–520.
Maikawa, C.L., Zimmerman, N., Ramos, M., Shah, M., Wallace, J.S., Pollitt, K.J.G., 2018. Comparison of airway responses induced in a mouse model by the gas and particulate fractions of gasoline direct injection engine exhaust. Int. J. Environ. Res. Public Health 15, 429.
Massey, D.D., Kulshrestha, A., Taneja, A., 2013. Particulate matter concentrations and their related metal toxicity in rural residential environment of semi-arid region of India. Atmos. Environ. 67, 278–286.
Mohiuddin, K., Strezov, V., Nelson, P.F., Evans, T., 2016. Bonding structure and mineral analysis of size resolved atmospheric particles nearby steelmaking industrial sites in Australia. Aerosol Air Qual. Res. 16, 1638–1650.
Oeder, S., Kanashova, T., Sippula, O., Sapcariu, S.C., Streibel, T., Arteaga-Salas, J.M., Passig, J., Dilger, M., Paur, H.R., Schlager, C., Mulhopt, S., Diabate, S., Weiss, C., Stengel, B., Rabe, R., Harndorf, H., Torvela, T., Jokiniemi, J.K., Hirvonen, M.R., Schmidt-Weber, C., Traidl-Hoffmann, C., Berube, K.A., Wlodarczyk, A.J., Prytherch, Z., Michalke, B., Krebs, T., Prevot, A.S.H., Kelbg, M., Tiggesbaumker, J., Karg, E., Jakobi, G., Scholtes, S., Schnelle-Kreis, J., Lintelmann, J., Matuschek, G., Sklorz, M., Klingbeil, S., Orasche, J., Richthammer, P., Muller, L., Elsasser, M., Reda, A., Groger, T., Weggler, B., Schwemer, T., Czech, H., Ruger, C.P., Abbaszade, G., Radischat, C., Hiller, K., Buters, J.T.M., Dittmar, G., Zimmermann, R., 2015. Particulate matter from both heavy fuel oil and diesel fuel shipping emissions show strong biological effects on human lung cells at realistic and comparable in vitro exposure conditions. PLoS One 10 (6), e0126536.
Oh, N., Park, J.H., 2014. Endocytosis and exocytosis of nanoparticles in mammalian cells. Int. J. Nanomed. 9, 51–63.
Park, S.K., Jeon, Y.M., Son, B.S., Youn, H.S., Lee, M.Y., 2011. Proteomic analysis of the differentially expressed proteins by airborne nanoparticles. J. Appl. Toxicol. 31, 463–470.
Pelucchi, C., Negri, E., Gallus, S., Boffetta, P., Tramacere, I., La Vecchia, C., 2009. Long-term particulate matter exposure and mortality: a review of European epidemiological studies. BMC Public Health 9, 453.
Putaud, J.P., Raes, F., Van Dingenen, R., Bruggemann, E., Facchini, M.C., Decesari, S., Fuzzi, S., Gehrig, R., Huglin, C., Laj, P., Lorbeer, G., Maenhaut, W., Mihalopoulos, N., Mulller, K., Querol, X., Rodriguez, S., Schneider, J., Spindler, G., ten Brink, H., Torseth, K., Wiedensohler, A., 2004. European aerosol phenomenology-2: chemical characteristics of particulate matter at kerbside, urban, rural and background sites in Europe. Atmos. Environ. 38, 2579–2595.
Qi, Z.H., Song, Y.Y., Ding, Q.Q., Liao, X.L., Li, R.J., Liu, G.G., Tsang, S., Cai, Z.W., 2019. Water soluble and insoluble components of $PM_{2.5}$ and their functional cardiotoxicities on neonatal rat cardiomyocytes in vitro. Ecotoxicol. Environ. Saf. 168, 378–387.
Rodriguez-Cotto, R.I., Ortiz-Martinez, M.G., Rivera-Ramirez, E., Mateus, V.L., Amaral, B.S., Jimenez-Velez, B.D., Gioda, A., 2014. Particle pollution in Rio de Janeiro, Brazil: increase and decrease of pro-inflammatory cytokines IL-6 and IL-8 in human lung cells. Environ. Pollut. 194, 112–120.
Sanchez-Soberon, F., Cuykx, M., Serra, N., Linares, V., Belles, M., Covaci, A., Schuhmacher, M., 2018. In-vitro metabolomics to evaluate toxicity of particulate matter under environmentally realistic conditions. Chemosphere 209, 137–146.
Shi, G., Chen, Z., Teng, J., Bi, C., Zhou, D., Sun, C., Li, Y., Xu, S., 2012. Fluxes, variability and sources of cadmium, lead, arsenic and mercury in dry atmospheric depositions in urban, suburban and rural areas. Environ. Res. 113, 28–32.
Steenhof, M., Gosens, I., Strak, M., Godri, K.J., Hoek, G., Cassee, F.R., Mudway, I.S., Kelly, F.J., Harrison, R.M., Lebret, E., Brunekreef, B., Janssen, N.A.H., Pieters, R.H.H., 2011. In vitro toxicity of particulate matter (PM) collected at different sites in The Netherlands is associated with PM composition, size fraction and oxidative potential - the RAPTES project. Part. Fibre Toxicol. 8, 26.
Takeichi, M., 1995. Morphogenetic roles of classic cadherins. Curr. Opin. Cell Biol. 7, 619–627.
Theocharis, A.D., Skandalis, S.S., Neill, T., Multhaupt, H.A.B., Hubo, M., Frey, H., Gopal, S., Gomes, A., Afratis, N., Lim, H.C., Couchman, J.R., Filmus, J., Sanderson, R.D., Schaefer, L., Iozzo, R.V., Karamanos, N.K., 2015. Insights into the key roles of proteoglycans in breast cancer biology and translational medicine. Biochim. Biophys. Acta 1855, 276–300.

Vaccari, M., Mascolo, M.G., Rotondo, F., Morandi, E., Quercioli, D., Perdichizzi, S., Zanzi, C., Serra, S., Poluzzi, V., Angelini, P., Grilli, S., Colacci, A., 2015. Identification of pathway-based toxicity in the BALB/c 3T3 cell model. Toxicol. In Vitro 29, 1240–1253.

Velali, E., Papachristou, E., Pantazaki, A., Choli-Papadopoulou, T., Argyrou, N., Tsourouktsoglou, T., Lialiaris, S., Constantinidis, A., Lykidis, D., Lialiaris, T.S., Besis, A., Voutsa, D., Samara, C., 2016a. Cytotoxicity and genotoxicity induced in vitro by solvent-extractable organic matter of size-segregated urban particulate matter. Environ. Pollut. 218, 1350–1362.

Velali, E., Papachristou, E., Pantazaki, A., Choli-Papadopoulou, T., Planou, S., Kouras, A., Manoli, E., Besis, A., Voutsa, D., Samara, C., 2016b. Redox activity and in vitro bioactivity of the water-soluble fraction of urban particulate matter in relation to particle size and chemical composition. Environ. Pollut. 208, 774–786.

Voutsa, D., Samara, C., 2002. Labile and bioaccessible fractions of heavy metals in the airborne particulate matter from urban and industrial areas. Atmos. Environ. 36, 3583–3590.

Vuong, N.Q., Breznan, D., Goegan, P., O'Brien, J.S., Williams, A., Karthikeyan, S., Kumarathasan, P., Vincent, R., 2017. In vitro toxicoproteomic analysis of A549 human lung epithelial cells exposed to urban air particulate matter and its water-soluble and insoluble fractions. Part. Fibre Toxicol. 14, 39.

Wang, R.W., Liu, G.J., Sun, R.Y., Yousaf, B., Wang, J.Z., Liu, R.Q., Zhang, H., 2018. Emission characteristics for gaseous- and size-segregated particulate PAHs in coal combustion flue gas from circulating fluidized bed (CFB) boiler. Environ. Pollut. 238, 581–589.

Wong, A., Zhang, S.F., Mordue, D., Wu, J.M., Zhang, Z.T., Darzynkiewicz, Z., Lee, E.Y.C., Lee, M.Y.W.T., 2013. PDIP38 is translocated to the spliceosomes/nuclear speckles in response to UV-induced DNA damage and is required for UV-induced alternative splicing of MDM2. Cell Cycle 12, 3184–3193.

Yi, S., Zhang, F., Qu, F., Ding, W.J., 2014. Water-insoluble fraction of airborne particulate matter (PM_{10}) induces oxidative stress in human lung epithelial A549 cells. Environ. Toxicol. 29, 226–233.

Zanobetti, A., Dominici, F., Wang, Y., Schwartz, J.D., 2014. A national case-crossover analysis of the short-term effect of $PM_{2.5}$ on hospitalizations and mortality in subjects with diabetes and neurological disorders. Environ. Health 13, 38.

Zhang, P., Tu, B., Wang, H., Cao, Z.Y., Tang, M., Zhang, C.H., Gu, B., Li, Z.M., Wang, L.N., Yang, Y., Zhao, Y., Wang, H.Y., Luo, J.Y., Deng, C.X., Gao, B., Roeder, R.G., Zhu, W.G., 2014. Tumor suppressor p53 cooperates with SIRT6 to regulate gluconeogenesis by promoting FoxO1 nuclear exclusion. P. Natl. Acad. Sci. USA 111, 10684–10689.

Zhang, Y.P., Chen, J., Yang, H.N., Li, R.J., Yu, Q., 2017. Seasonal variation and potential source regions of $PM_{2.5}$-bound PAHs in the megacity Beijing, China: impact of regional transport. Environ. Pollut. 231, 329–338.

Zhang, Z.J., Tang, Z.J., Zhu, Z.Y., Cao, Z.M., Chen, H.J., Zheng, W.J., Hu, X., Lian, H.Z., Mao, L., 2018. The time-dependent cellular response mechanism upon exposure to zinc oxide nanoparticles. J. Nano Res. 20, 263.

Zhao, C., Niu, M.Y., Song, S.Y., Li, J., Su, Z.L., Wang, Y., Gao, Q., Wang, H.W., 2019. Serum metabolomics analysis of mice that received repeated airway exposure to a water-soluble $PM_{2.5}$ extract. Ecotoxicol. Environ. Saf. 168, 102–109.

Zhao, W.J., Song, Q., Wang, Y.H., Li, K.J., Mao, L., Hu, X., Lian, H.Z., Zheng, W.J., Hua, Z.C., 2014. Zn-responsive proteome profiling and time-dependent expression of proteins regulated by MTF-1 in A549 Cells. PLoS One 9 (8), e105797.

Zhao, W.J., Song, Q., Zhang, Z.J., Mao, L., Zheng, W.J., Hu, X., Lian, H.Z., 2015. The kinetic response of the proteome in A549 cells exposed to $ZnSO_4$ Stress. PLoS One 10 (7), e0133451.

Zhao, W.J., Zhang, Z.J., Zhu, Z.Y., Song, Q., Zheng, W.J., Hu, X., Mao, L., Lian, H.Z., 2018. Time-dependent response of A549 cells upon exposure to cadmium. J. Appl. Toxicol. 38, 1437–1446.